

Chandra imaging of the complex X-ray core of the Perseus cluster

A. C. Fabian,¹★ J. S. Sanders,¹ S. Ettori,¹ G. B. Taylor,² S. W. Allen,¹ C. S. Crawford,¹
K. Iwasawa,¹ R. M. Johnstone¹ and P. M. Ogle³

¹*Institute of Astronomy, Madingley Road, Cambridge CB3 0HA*

²*National Radio Astronomy Observatory, PO Box 0, Socorro, NM 87801, USA*

³*Center for Space Research, Massachusetts Institute of Technology, Cambridge, MA 02139, USA*

Accepted 2000 July 27. Received 2000 July 25; in original form 2000 May 24

ABSTRACT

We report subarcsec-resolution X-ray imaging of the core of the Perseus cluster around the galaxy NGC 1275 with the *Chandra X-ray Observatory*. The *ROSAT*-discovered holes associated with the radio lobes have X-ray bright rims which are cooler than the surrounding gas and not a result of shocks. The holes themselves may contain some hotter gas. We map strong photoelectric absorption across the northern lobe and rim owing to a small infalling irregular galaxy, known as the high-velocity system. Two outer holes, one of which was previously known, are identified with recently found spurs of low-frequency radio emission. The spiral appearance of the X-ray cooler gas and the outer optical parts of NGC 1275 may be due to angular momentum in the cooling flow.

Key words: galaxies: clusters: individual: Perseus – cooling flows – galaxies: individual: NGC 1275 – X-rays: galaxies.

1 INTRODUCTION

The Perseus cluster, Abell 426, at a redshift $z = 0.0183$ or distance of about 100 Mpc is the brightest cluster in the sky in X-rays. It hosts the nearest large cooling flow (e.g. Fabian et al. 1981; Allen et al. 1992; Fabian et al. 1994). X-ray analysis of *ASCA* spectra indicates that the mass deposition rate is about $300 M_{\odot} \text{ yr}^{-1}$ (Allen et al. 2000). At the centre is the galaxy NGC 1275, surrounded by a spectacular low-ionization, emission-line nebula (Lynds 1970). The nucleus powers the radio source 3C 84 (Pedlar et al. 1990). *ROSAT* High Resolution Imager (HRI) images of the central region around NGC 1275 show two ‘holes’ in the X-ray emission coincident with the 0.5-arcmin-sized radio lobes of 3C 84 (Böhringer et al. 1993). The overlap of the holes with both radio and optical images of NGC 1275 has been discussed further by McNamara, O’Connell & Sarazin (1996), and the overall X-ray structure has been discussed by Churazov et al. (2000). Here we present *Chandra* observations of the core of the Perseus cluster using the ACIS-S detector, covering the energy range 0.5–7 keV.

2 THE X-RAY IMAGE

The core of the Perseus cluster was observed with the *Chandra X-ray Observatory* (Weisskopf et al. 2000) on 2000 January 29 for 24 453 s. The 0.5–7 keV band image of the innermost 6.5 arcmin (195 kpc) diameter region centred on NGC 1275 is

★ E-mail: acf@ast.cam.ac.uk

shown in Fig. 1. It has been exposure-map corrected, chiefly to remove the effects of nodal readout boundary structures. These mainly consist of two rows of pixels running from close to the nucleus out to the west (PA 260°).

The holes in the emission associated with the inner radio lobes of 3C 84 are clearly seen, as well as the larger hole to the north-west, known from *Einstein Observatory* images (Fabian et al. 1981; Branduardi-Raymont et al. 1981). The inner radio holes in the 0.5–7 keV image are deep with a central surface brightness (20–25 count arcsec⁻² for the southern hole and 15–30 count arcsec⁻² for the northern hole) comparable to those of regions generally of twice their radius (Fig. 2). The holes are surrounded by bright rims at about 60 to 30 count arcsec⁻² to the north and 40 to 30 count arcsec⁻² in the south. The simplest interpretation is that the rims of bright emission are shells enclosing the holes. A bright patch of emission to the east, about 40 by 15 arcmin², yields about 50–80 count arcsec⁻². The outer north-western hole is at 7 count arcsec⁻² and is surrounded by emission at about 23 to 17 count arcsec⁻².

The nucleus of NGC 1275 appears slightly extended and is spectrally hard in our images. (Correction for the nodal readout boundary structures, one of which passes close to the nucleus, has artificially increased the apparent size of the nucleus in the images shown here.) We defer discussion of its structure and detailed spectrum to future work.

3 X-RAY COLOUR ANALYSIS

We have made soft (0.5–1 keV), medium (1–2 keV) and hard

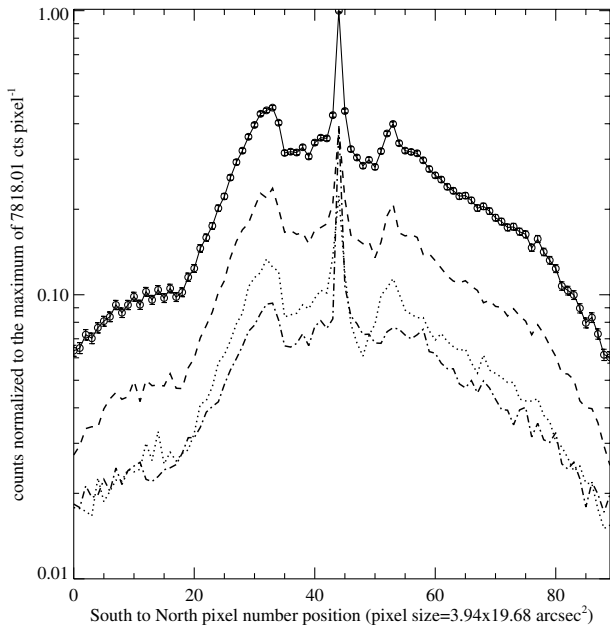


Figure 2. Profile from south to north across the centre of the Perseus cluster. The top curve is from the 0.5–7 keV band, with the 1–2, 0.5–1 and 2–7 keV profiles lying below (upper to lower).

(2–7 keV) X-ray maps in order to study the X-ray colours of the inner parts of the cluster. They have been simply superimposed using the software tool GIMP to provide the colour image shown in Fig. 3. It is immediately seen that there are no strong colour gradients, apart from some patches of hard emission (blue) across the northern hole and its western rim. The holes are clearly not due to absorption (or they would appear blue in Fig. 3) and the rims are not hard but moderately soft, of the same colours as the western bright patch. Inspection of separate colour images bears this last result out: the rims are not distinguishable as sharp features on a 3–7 keV image. They are therefore not shock features, contrary to the prediction of Heinz, Reynolds & Begelman (1998), and the holes are not expanding supersonically.

The patchy absorption structure seen across the northern hole and its western rim is clearly seen in Fig. 4, which covers the 0.5–1 keV band. This structure coincides in position and length with the high-velocity emission-line nebulosity seen to the north of NGC 1275 (Unger et al. 1990, and references therein). This gas is thought to be associated with a small irregular galaxy falling into the centre of the Perseus cluster at a relative velocity of 3000 km s^{-1} . Since it is seen in absorption at 21 cm (de Young, Roberts & Saslaw 1973) and Ly α (Briggs, Snijders & Boksenberg 1982), it must lie in front of NGC 1275. Our discovery of extended X-ray absorption by this galaxy means that it must lie well in front of the innermost regions, or such deep absorption features would not be apparent. Without knowledge of the detailed geometry of the holes and emission features, we cannot establish any precise estimate of its radial distance from the centre, but note that the count rate at the bottom of the absorption patches is lower than anywhere else within the inner 2-arcmin radius. This suggests that the infalling galaxy may be more than 60 kpc from the cluster centre. The westernmost part of the absorption structure appears to be surrounded by brighter X-ray emission (Figs 4 and 5). This could be shocked gas within the infalling galaxy.

In order to quantify the temperature and absorption column

density structure in the inner parts of the image, we have compared colour ratio images with tables of theoretical colour ratios. First we have adaptively binned the data, after background subtraction, using a local bin size which approximately equalizes the joint fractional error per bin (over all colours) across the image. The counts from the three bands in each bin then provide the colour ratios. The tables were predicted using the appropriate response matrices and auxiliary responses for the S3 detector and the MEKAL spectral code in XSPEC. A metallicity of 0.4 times the cosmic value for all bins was assumed. Temperature and column density maps were produced by least-squares fitting of the observed colour ratios to the tables. An adaptively smoothed (Ebeling, White & Rangarajan 2000) image is included in Fig. 5 to illustrate the various features on the scale of the temperature and column density maps. The results confirm and quantify the appearance obtained from inspection of the separate maps. The brighter emission arises from gas that is at about 2.7-keV temperature, less than half that of the outer gas which has a temperature of about 6.5 keV, in good agreement with the ASCA results (e.g. Allen et al. 2000). The infalling galaxy has a mean excess column density of about 10^{21} cm^{-2} which, over the region covered, corresponds to any absorbing mass of about $2 \times 10^9 M_{\odot}$ at cosmic abundance.

The maps were then converted into (hot) electron density, pressure and radiative cooling time maps (Fig. 6) using the surface brightness of the 1–2 keV map (the band with the highest count rate). The XSPEC-constructed tables enable the spectral normalization of the assumed MEKAL models to be obtained and thereby the emission measure of each pixel. We then assumed that the path length through the emitting gas is equal to the radius from the nucleus of that pixel, in order to convert the emission measure into a density. This is a gross assumption, approximately correct for a symmetrical, highly peaked emission profile. Despite the holes etc. in our image, it should give a rough indication of the gas properties (the density depends on the inverse square root of the path length). We note that the pressure inferred for the gas within a few kpc of the nucleus agrees with that determined from the optical [S II] line ratio by Johnstone & Fabian (1988) and Heckman et al. (1989).

4 OPTICAL AND RADIO

The soft X-ray image is shown next to an optical *B*-band image in Fig. 4. The *B*-band image was constructed from data obtained from the Isaac Newton Group Archive. The image is the combination of images taken on 1997 December 25 and 1998 August 22 with the Jacobus Kapteyn Telescope (JKT) using the Tek1024 detector, with a total exposure time of 17.7 ks. The data have been bias-subtracted and flat-fielded before being combined. The correspondence between the soft X-ray absorption structure and the high-velocity system in the optical image is good. There are no other obvious optical structures correlated with the X-ray image.

VLA observations at a frequency of 1.4 GHz were combined from several runs of 3–10 h duration, each taken between 1989 and 1999 in the A, B and C configurations. The resulting radio image, shown in Fig. 7, has been restored with a 5-arcsec synthesized beam. Contour levels start at 1 mJy beam^{-1} and increase by factors of 2 to just below the peak of $21.7 \text{ Jy beam}^{-1}$.

We note that the steepest part of the radio contours abuts the brightest part of the eastern patch.

5 DISCUSSION

The overall X-ray appearance of the core of the Perseus cluster is of a broadly circularly symmetric peak centred on NGC 1275. The gas temperature decreases inward with radius, from about 6.5 to less than 3 keV, as determined from the colour ratios assuming a single-phase gas. The radiative cooling time of the gas across the bright patch south-east of the nucleus is about 10^8 yr. Therefore, unless there is a balance with heating, the gas is part of a cooling flow (see Fabian 1994) and is expected to be multiphase, with the measured temperatures being an emission-weighted mean. The radiative cooling time is less than 6×10^9 yr across the whole of the images shown.

The radio lobes of 3C 84 occupy holes in the X-ray emission. The simplest interpretation of the low surface brightness is that they are devoid of X-ray gas and have pressure support from cosmic rays and magnetic fields. However, there may be hotter gas in the holes, and indeed we find that the pressure map shows little evidence for the holes (the temperature map, Fig. 5, indicates 4–5 keV for the holes; a result which is highly geometry-dependent). The data are consistent with the holes being filled with pressure-supporting hotter gas. Future work involving detailed deprojection and spectral fits to the data will enable this possibility to be carefully tested.

The composition of the radio lobes is important in determining the energy content of the radio source and, using a synchrotron age, the mean power output of the central engine. We have already noted that there is no evidence for shocks, so any expansion is subsonic. If the holes contain only magnetic fields and cosmic rays then the energy is approximately $P\Delta V \approx 8 \times 10^{58}$ erg (assuming that the holes are spheres of radius 6 kpc each). A similar amount of work must have been done in making the holes. That work probably causes a very low-frequency sound wave to propagate out from the hole region and dissipate beyond the cluster core. There is no reason that it should lead to local heating. The age of the inner holes is unclear but probably of the order of 10^{7-8} yr, from synchrotron ageing estimates and also buoyancy considerations (Pedlar et al. 1990; McNamara et al. 2000; Churazov et al. 2000). The mean power of the nucleus is then $\sim 10^{44-45}$ erg s $^{-1}$.

If the holes are just apparent and filled with hotter, lower surface brightness gas than the rims, then it is difficult to estimate the energy of the radio source. A probable lower estimate is the minimum-energy one of Pedlar et al. (1990), which implies a pressure for the relativistic fluid about 10 times less than the local gas pressure. The magnetic fields and/or cosmic rays need not be space-filling; pressure balance is obtained if they occupy about 2 per cent of the volume. The relativistic fluid may still have a large covering factor and just pushes denser, cooler gas clouds out of the way, so that they accumulate at the edge of the lobes, forming the bright rims. The brightness of the rims relative to the surrounding region is consistent with this hypothesis (i.e. $\Delta S/S \sim R/\Delta R$, where S and R are surface brightness and radius, respectively).

The origin of the outer north-west hole is unclear. It could, as suggested by Churazov et al. (2000), be a buoyant old radio lobe, or lobes, produced by the central engine in NGC 1275. If so then it must have considerable surface tension, presumably due to ordered magnetic fields, in order that it has not fallen apart. Perhaps the galaxy is moving slowly to the south-east and shed this lobe in the past. Such a scenario could also account for the western bright patch as being where cooler X-ray-emitting clouds of gas are swept up by the radio lobes.

The situation is clarified somewhat by the recent low-frequency (74 MHz) radio image of Blundell, Kassim & Perley (2000), which shows a spur of radio emission out to the position of the outer hole [there is also some structure in the maps of Pedlar et al. (1990) in this position]. The low-frequency map also shows a spur to the south-south-east, in the direction of another hole seen in Fig. 5. Such low-frequency radio emission is likely to originate from the oldest electron populations, thereby supporting the idea that the spurs point to fossil radio lobes now devoid of energetic electrons.

Of course, some of the apparent displacement of the outer holes from the present jet (north–south) axis may be due to motion of the gas, rather than the galaxy. If there is slow rotation of the gas then this could explain the ‘swirly’ appearance of the outer gas in Fig. 1 (noted by Churazov et al. 2000). It could be the remains of an earlier cooler subcluster which merged with the cluster core. The impression of a spiral structure winding inward in a clockwise sense is reinforced by similar structures apparent in optical images (see e.g. Carlson et al. 1998). We note that such an overall structure is consistent with a cooling flow if the gas has some angular momentum which is roughly conserved as the slow inflow proceeds. The streamlines of the flow will be spiral rather than radial lines. These can then become apparent if the gas at ~ 50 -kpc radius has some large-scale inhomogeneity in the form of a wider spread of denser, cooler gas over, say, one quadrant. As the gas cools the denser gas cools fastest, and as it flows inward creates an X-ray-bright and cooler spiral. The optical spiral is explained by star formation from the cooled gas.

Neither movement of gas nor movement of the galaxy, however, obviously explains the outer southern hole being along the present jet axis. The outer holes may result as much from previous beaming directions of the central engine as from its displacement. The situation resembles that around M87, as found by Böhringer et al. (1995) and most recently by Owen, Eilek & Kassim (1999). If this explanation is correct then it argues against rapid spin of the central black hole being the origin of the jets. The outer holes nevertheless do provide direct evidence that the central radio source is sporadic and had earlier outbursts.

ACKNOWLEDGMENTS

ACF is grateful to NASA for the opportunity to participate as an InterDisciplinary Scientist, and to the *Chandra* project for such a superb instrument. ACF, CSC and SWA thank the Royal Society for support.

REFERENCES

- Allen S. W., Fabian A. C., Edge A. C., Johnstone R. M., Nulsen P. E. J., 1992, MNRAS, 254, 51
- Allen S. W., Fabian A. C., Johnstone R. M., Nulsen P. E. J., Arnaud K. A., 2000, MNRAS, submitted (astro-ph/9910188)
- Blundell K., Kassim N., Perley R., 2000, ASP Conf. Ser., Astron. Soc. Pac., San Francisco, in press (astro-ph/0004005)
- Böhringer H., Voges W., Fabian A. C., Edge A. C., Neumann D. M., 1993, MNRAS, 264, L25
- Böhringer H., Nulsen P. E. J., Braun R., Fabian A. C., 1995, MNRAS, 274, L67
- Branduardi-Raymont G., Fabricant D., Feigelson E., Gorenstein P., Grindlay J., Soltan A., Zamorani G., 1981, ApJ, 248, 55
- Briggs S. A., Snijders M. A. J., Boksenberg A., 1982, Nat, 300, 336
- Carlson M. N. et al., 1998, AJ, 115, 1778

- Churazov E., Forman W., Jones C., Böhringer H., 2000, *A&A*, 356, 788
de Young D. S., Roberts M. S., Saslaw W. C., 1973, *ApJ*, 185, 809
Ebeling H., White D. A., Rangarajan V., 2000, *MNRAS*, submitted
Fabian A. C., 1994, *ARA&A*, 32, 277
Fabian A. C., Hu E. M., Cowie L. L., Grindlay J., 1981, *ApJ*, 248, 47
Fabian A. C., Arnaud K. A., Bautz M. W., Tawara Y., 1984, *ApJ*, 436, L63
Heckman T. M., Baum S. A., van Breugel W. J. M., McCarthy P., 1989, *ApJ*, 338, 48
Heinz S., Reynolds C. S., Begelman M. C., 1998, *ApJ*, 501, 126
Johnstone R. M., Fabian A. C., 1988, *MNRAS*, 233, 581
Lynds C. R., 1970, *ApJ*, 159, L151
McNamara B. R., O'Connell R. W., Sarazin C. L., 1996, *AJ*, 112, 91
McNamara B. R. et al., 2000, *ApJ*, 534, 135
Owen F., Eilek J., Kassim N., 1999, in Böhringer H., Feretti L., Schuecker P., eds, *MPE Report 271, Diffuse Thermal and Relativistic Plasmas in Galaxy Clusters*. MPE, Garching
Pedlar A., Ghataure H. S., Davies R. D., Harrison B. A., Perley R., Crane P. C., Unger S. W., 1990, *MNRAS*, 246, 477
Unger S. W., Taylor K., Pedlar A., Ghataure H. S., Penston M. V., Robinson A., 1990, *MNRAS*, 242, 33P
Weisskopf M. C., Tananbaum H. D., Van Spebroeck L. P., O'Dell S. L., 2000, *Proc. SPIE*, 4012, in press (astro-ph/0004127)

This paper has been typeset from a $\text{\TeX}/\text{\LaTeX}$ file prepared by the author.

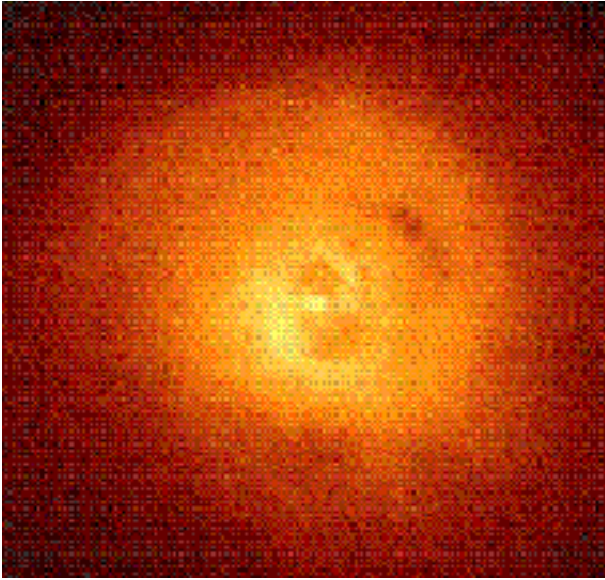


Figure 1. *Chandra* image of the central, 6.5 arcmin wide, field of the Perseus cluster in the 0.5–7 keV energy band. The pixel size is 1 arcsec; north is to the top and east to the left.

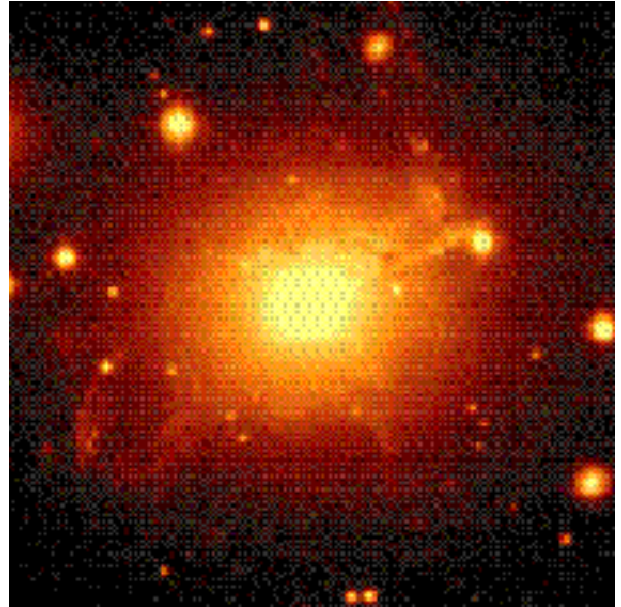
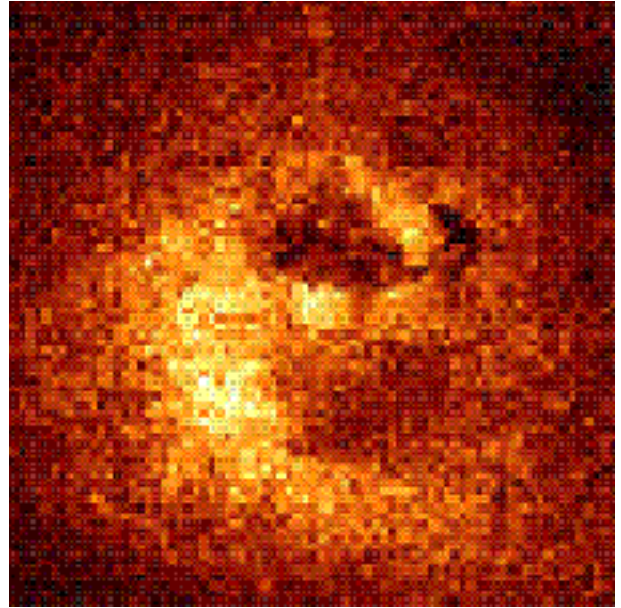


Figure 4. Soft X-ray (0.5–1 keV) map (above) showing well the absorption structure, and a *B*-band optical image from the JKT (below) on the same scale. The images are 150×150 arcsec².

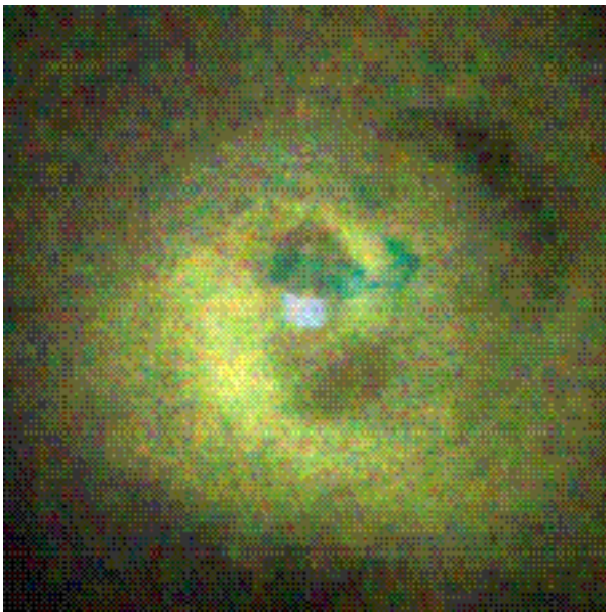


Figure 3. X-ray colour image composed of exposure-corrected 0.5–1 keV (red), 1–2 keV (green) and 2–7 keV (blue) images. The image is 3.5 arcmin square.

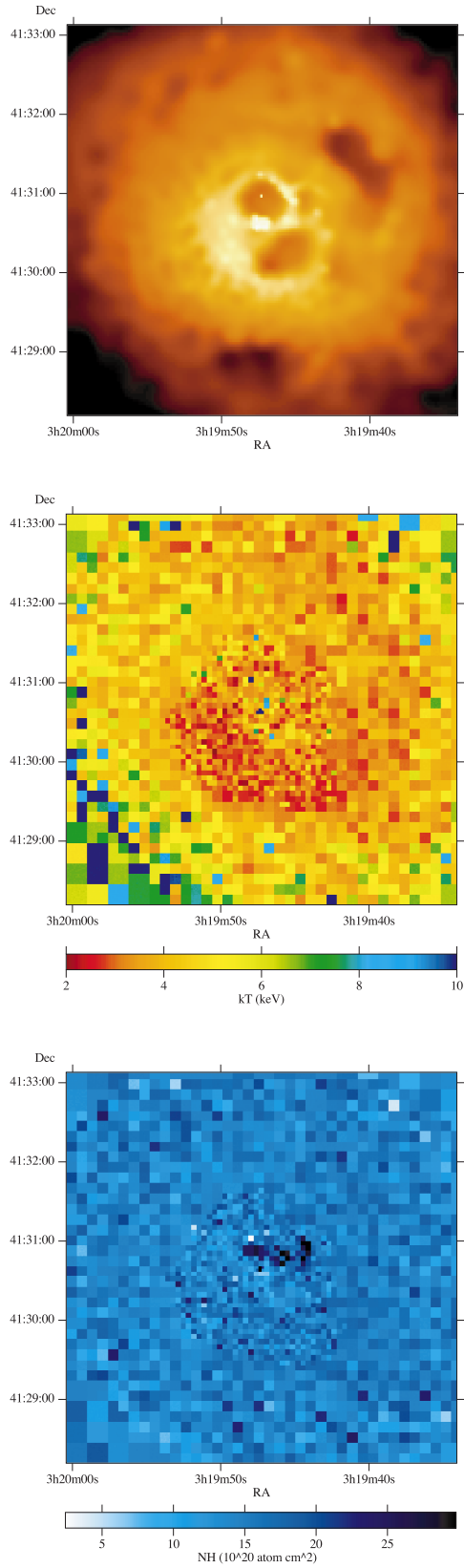


Figure 5. Temperature (middle) and column density (bottom) maps from adaptively binned images with an adaptively smoothed 0.5–7 keV image (above). View the top image along PA 333° for a surprise.

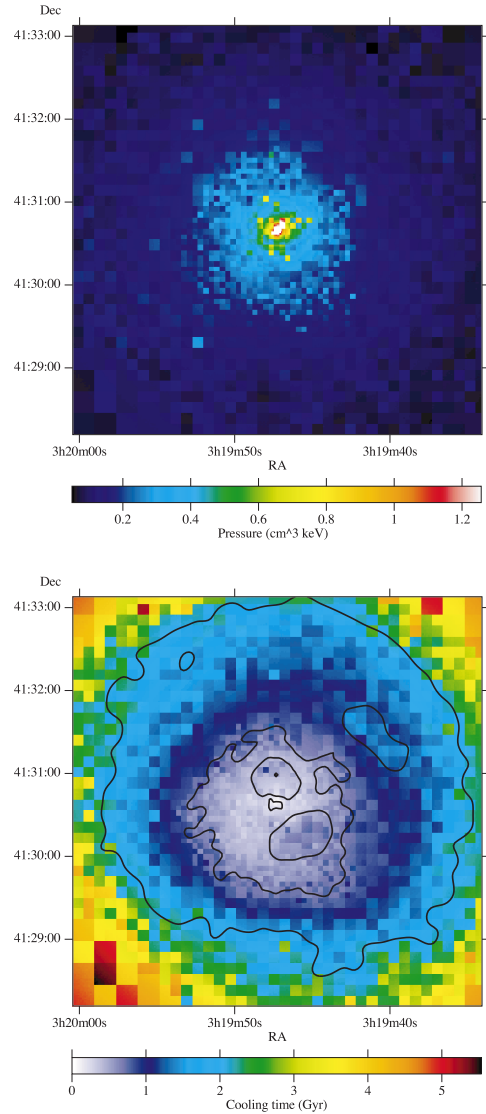


Figure 6. Pressure (electron density times temperature; top) and radiative cooling time (in Gyr from bremsstrahlung formula; bottom) from the maps in Fig. 6.

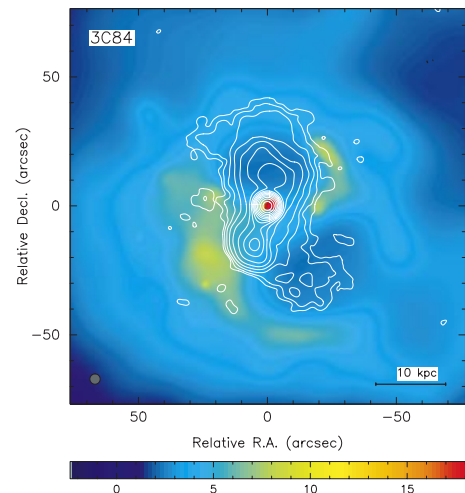


Figure 7. Radio image overlay; see text for details.